Available online at www.sciencedirect.com
ScienceDirect
Ceramics International 37 (2011) 3217–3227
CERAMICS INTERNATIONAL
www.elsevier.com/locate/ceramint

Experimental study of the thermo-mechanical behaviour of alumina-silicate refractory materials based on a mixture of Algerian kaolinitic clays

B. Amrane [a,b,c,e], E. Ouedraogo [a,b,c,*], B. Mamen [a,b,c], S. Djaknoun [d], N. Mesrati [e]

[a] Grenoble-INP, Laboratoire 3SR, France
[b] UJF, Laboratoire 3SR, France
[c] CNRS UMR 5521 Laboratoire 3SR, BP53, 38041 Grenoble, cedex 9, France
[d] Laboratoire de Mécanique Avancée (LMA), FGM&GP, USTHB, BP 32, El-Alia, 1611 Alger, Algeria
[e] Laboratoire Sciences et Génie des Matériaux (LSGM), Ecole Nationale Polytechnique d'Alger, 10 avenue Hassen Badi El Harrach ALGER, Algeria

Received 2 August 2010; received in revised form 19 February 2011; accepted 20 March 2011
Available online 27 May 2011

Abstract

In the framework of a general study carried out on the thermo-mechanical behaviour of refractory products made from Algerian refractory clays, silica–alumina bricks based on a mixture of halloysite from Djebel Debbagh and kaolin from Tamazert were studied. The material's initial chemical composition and physical properties are reported. Uniaxial compression and three-point bending tests were performed under temperature conditions from room temperature to 1200 °C on representative specimens cut from the bricks. The evolution of the material's resistance in tension and compression as of its modulus of elasticity with testing temperature is reported. The thermal expansion of the material was investigated as were optical and SEM micrographs at various temperatures. The evolution of the material rheological behaviour from quasi-brittle, between room and 900 °C, to viscous at higher temperatures was shown by both bending and compression tests. The general behaviour of the material with increasing temperature was analysed through the various microstructure investigations and the presence of micro-cracking induced by the differential expansions of the multiple phases in presence.

Keywords: E. Refractories; Alumina-silicate; Thermo-mechanical properties; Kaolinitic clays; High temperatures

1. Introduction

Alumina silicate refractories are extensively used in the metallurgical, ceramic and glass industries, representing an important material in the overall refractory market [1,2]. These materials are made primarily from refractory and kaolinitic clays, which are used both in crude and grog forms. Chamotte (fired refractory clay) transforms refractories into stable high temperature compounds, and limits the shrinkage and cracking during the drying and firing steps [3,4]. In the crude unfired form, the clays act as a binder. Silica–alumina refractory materials generally have a heterogeneous microstructure with a large grain size distribution and high porosity [5–7].

The mineralogical composition of refractory materials based on kaolinitic clays consists of mullite ($3Al_2O_3$ $2SiO_2$) and silica, both in crystalline form (quartz or cristobalite) and in the amorphous phase. The mullite phase results from the transformation of kaolinite [Al_2O_3 $2SiO_2{\cdot}2H_2O$] during high temperature thermal cycle [5]. Mullite-based ceramics have important chemical physical properties, including good resistance to corrosion and creep, are high temperature materials and exhibit a low thermal expansion coefficient [5,8–10]. These advantages confer to mullite-based refractories the ability to bear severe service conditions encountered in a variety of applications. The vitreous phase resulting from the reactions between free silica and alkalines governs the thermo-mechanical behaviour of alumina-silicate refractory materials, limiting their use at high temperatures [2,11]. The content of the vitreous phase varies according to the raw materials, chemical compositions and firing temperature.

Hallohysite from Djebbel Debbagh (DD3) and kaolin from Tamazert (KT) are the main refractory clays deposits mined in Algeria for manufacturing of silica–alumina refractories. These products are commonly used in the ceramics industry to

* Corresponding author at: Laboratoire 3SR, UMR5521,BP 53, 38041 Grenoble cedex 09, France. Tel.: +33 476 82 52 97.
E-mail address: Evariste.Ouedraogo@grenoble-inp.fr (E. Ouedraogo).

0272-8842/$36.00 © 2011 Published by Elsevier Ltd and Techna Group S.r.l.
doi:10.1016/j.ceramint.2011.05.095

manufacture kilns, and as kiln furniture. However, these materials frequently deteriorate and wear because of thermal and mechanical constraints. This has a negative impact on the environment and on the price of finished products.

The long term aim of this study is to numerically simulate by finite element analysis the behaviour of bricks made from Algerian kaolin and refractory clay in service conditions. To do this, it is necessary to determine the material behaviour with increasing temperature, and to determine relevant equations and the evolution of the material's characteristic parameters with increasing temperature. Isothermal tests at various testing temperatures were conducted to accomplish this. The present study, which is an extension of a previous work devoted to the optimisation of the formulation and the conditions of elaboration [12], presents a thermo-mechanical characterisation of industrial silica–alumina refractory bricks made from a mixture of DD3 clay and KT. The thermal and physical properties of materials made with these clays were measured, and the microstructure characterised by XRD and by optical and SEM observations.

2. Materials and experimental procedure

2.1. Raw materials

The samples studied were made from a mixture selected among various compositions of DD3 clay and KT [12]. The clays were used in crude and calcinated forms (chamotte). DD3 clay was extracted from the quarry of Djebbel Debbagh, and is grey in colour and rich in alumina (Table 1). Its mineralogical composition consists mainly of hallohysite, kaolinite, and small quantities of quartz and non-plastic minerals such as goetite, calcite and plagioclase (Table 2). The grain size distribution of DD3 clay (Table 3) is predominately fine particles, which explains its high plasticity index (23). Because of the fine particles, this clay exhibits a pronounced linear shrinkage upon firing that causes large crack formation in fired products. KT clay is a white-coloured kaolin extracted from the deposit at Tamazert in the east of Algeria. It is rich in quartz (Tables 1 and 2) and has a low plasticity index (8) [12,13]. Because of its high content in kaolin, KT clay forms mullite when fired at high temperature. In this study, KT clay is mixed with DD3 clay to reduce shrinkage that especially leads to micro cracking. The fired grog added to the mixture was produced by firing DD3 at 1350 °C, and has the main characteristics shown in Tables 4 and 5, respectively.

Table 1
Chemical compositions of halloysite (DD3) and Kaolin (KT) [12,13].

Oxides	KT kaolin	Halloysite
SiO_2	69.86	39.87
Al_2O_3	19.29	38.36
Fe_2O_3	0.72	1.14
CaO	0.4	0.78
Na_2O	0.13	0.48
MnO	–	0.46
SO_3	0.03	0.45
MgO	0.4	0.24
K_2O	2.67	0.20
P_2O_5	–	0.02
TiO_2	0.4	0.02
Cr_2O_3	–	0.01
Calc. loss	6.31	17.27
Total	100.21	99.69

Table 2
Mineralogical composition of halloysite (DD3) and kaolin (KT) [12].

Clays	Major minerals	Minor minerals
DD3	Hallohysite, kaolinite, quartz	Calcite, goetite, plagioclase
KT kaolin	Kaolinite, muscovite, quartz	Goetite, rutile, feldspaths

Table 3
Particle size distribution of halloysite (DD3) and kaolin (KT) [12].

Clays	>1 mm (%)	0.01 à 1 mm (%)	<0.01 mm (%)
DD3	–	43.56	56.68
KT kaolin	27.15	52.85	27.15

2.2. Experimental techniques

2.2.1. Preparation of the bricks

To obtain representative material characteristics, fired samples were cut from commercial processed bricks that were a mixture of 30% wt. DD3, 35% wt. KT kaolin and 30% wt. chamotte. The optimum raw materials formulation was selected based on research conducted in a previous study [12], and represented the optimisation of physicochemical and thermal properties of sintered samples in that study.

Fired bricks, were produced commercially following the steps indicated in the flow chart of Fig. 1. The best production conditions from previous studies [12,13] were used. Mixed raw materials were moistened by adding 8% water by weight, then aged for 24 h. Test bricks, hereafter indicated as BSAA, were shaped by uniaxial compaction in a 100 t friction press under 35 MPa pressure. After drying at 60 °C, the bricks were fired at 1350 °C in a tunnel kiln in an oxidising environment for 33 h.

2.2.2. Characterisation of the bricks

The fired properties of the BSAA bricks were evaluated and are given in Table 6. The apparent density and open porosity were characterised by Archimedes' method, and the absolute density was determined using a helium picnometer. As the major properties of the refractory materials are intimately connected to their mineralogical composition, some samples were finely crunched and analysed by X-ray diffraction. The different phases formed after firing at 1350 °C were identified using the XPERT DATA COLLECTER software. The BSAA bricks microstructure was evaluated using scanning electron microscopy.

The thermal behaviour of BSAA samples was characterised up to 1200 °C according to the CHEVENARD method [14] by using a DI24 ADAMEL LHOMARGY dilatometer at a heating rate of 5 °C/min. The material's refractoriness was evaluated

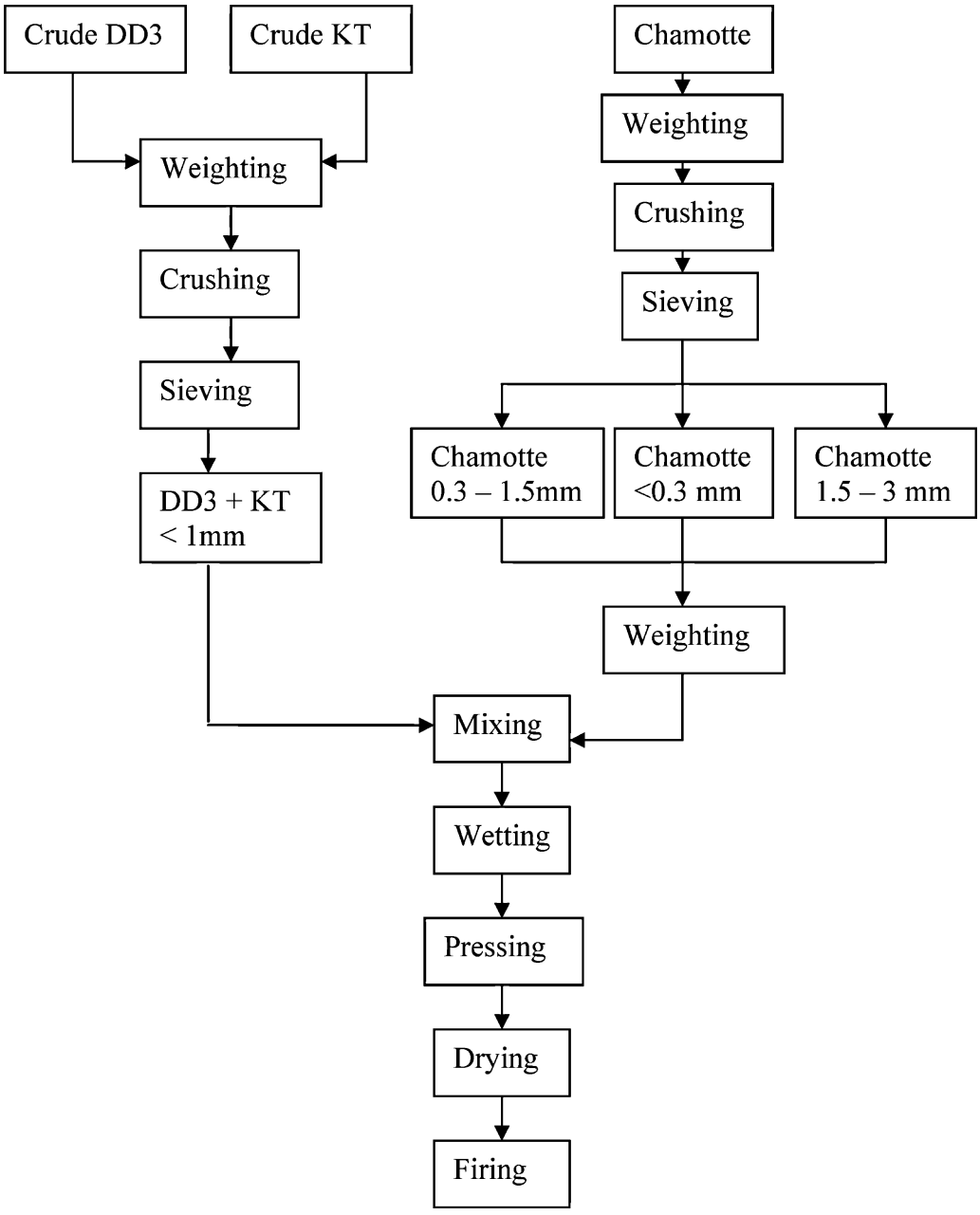

Fig. 1. Schematic representation of the manufacturing process of the BSAA bricks.

according to the DIN 51 730 standard [15] by measuring the melting point using macroscopic examination during heating.

Thermal shock tests were conducted according to the DIN 51 068 standard [16]. Samples were heated for 15 min at 950 °C and immediately quenched in room temperature water for 3 min. After drying for 2 h at 110 °C, the heating/quenching cycle was repeated until samples broke into several fragments.

2.2.3. Thermo-mechanical tests

Modulus of rupture mechanical testing was undertaken on high-temperature mechanical equipment specially built at the

Table 4
Mineralogical composition of the chamotte [12].

Constituents	Content (%)
Mullite	55
Quartz	10
Amorphous phase	32
Rutile	3

Table 5
Grain size distribution of the chamotte [12].

Grain size range	Content (%)
1.25–3 mm	26.06
0.315 à 1.25 mm	29.91
<0.315 mm	44.03

Table 6
Physical characteristics of BSAA bricks for 1350 °C prefired BSAA samples.

Characteristics	Values
Apparent density (g/cm^3)	2.00
Absolute density (g/cm^3)	2.60
Water absorption (%)	11.14
Open porosity (%)	22.34
Drying shrinkage (%)	0.65
Firing shrinkage (%)	1.24

3S-R Laboratory of the National Polytechnic Institute of Grenoble. This set-up consisted of a ZWICK Z400E electro-mechanical testing machine equipped with a PYROX 1600 °C electrical furnace and an exterior differential displacement measuring device. This set-up could be configured to perform uniaxial compression or three-point bending tests at various temperatures [17]. Compression and three-point bending specimens were made by sawing fired refractory bricks into desired shapes using a diamond saw. The cubic specimens for compression tests were then ground to ensure that the bearing faces were parallel within 30 μm. The specimens were calibrated to an initial height of 40 mm. Fig. 2 presents a view of a specimen placed in the experimental set-up. Three-point bending specimens consisted of bars with a square cross-section of 25 mm^2 and a length of 160 mm. The distance between bottom supports was 120 mm. The three local areas of the specimen bearing the test supports for three-point bending were treated to minimise initial geometrical defects. However, the initial positioning of the three-point bending apparatus was known to influence initial deflection of some of the load-deflection curves.

The uniaxial compression and three-point bending tests were carried out at ambient temperature, 500 °C, 700 °C, 900 °C, 1000 °C and 1200 °C. The loading procedure in both compression and three-point bending consisted of applying a preliminary load (2 KN in compression, 0.05 KN in flexion) at a rate of 0.5 mm/min to eliminate positioning defects of the specimens. For tests conducted at elevated temperatures, a standard thermal cycle was applied: samples were heated from room temperature to the target test temperature at the rate of 200 °C/h, followed by a 2 h hold at the test temperature before the mechanical loading was applied in isothermal conditions. After testing, samples were cooled to room temperature at a cooling rate of 150 °C/h. In both compression and three-point loading, the mechanical loading consisted of imposing a 0.1 mm/min displacement rate to the upper plunger. The two LVDT sensors of the differential displacement devices recorded the specimen's height variation in compression tests and the specimen's deflection in bending tests. It then became possible to display force–displacement or force–deflection curves generated from each test. The stresses and strains in compression tests were determined by the following equations:

$$\sigma = \frac{F}{a^2} \quad (1)$$

$$\varepsilon = \frac{i}{a} \quad (2)$$

where F is the actual measured load, a is the specimen side length and i is the average of the sensor indications. The evolution of the fracture surface vs. temperature was examined using an optical and scanning electron microscopy.

3. Results and discussion

3.1. Physical properties

The physical characteristics of the DD3 and KT test bricks averaged and labelled as BSAA bricks are listed in Table 6. Several studies carried out on refractory clay materials [3,6,11,18–20] showed that the sintered brick characteristics are influenced by the mineralogical composition of clays, the chamotte content and the firing temperature. In general, porosity increases with the inert grain ratio, whereas firing shrinkage decreases. The firing temperature of brick made using the clays also influences properties, with higher temperatures enhancing densification by the formation of a liquid phase. The liquid phase is formed by reactions that occur

Fig. 2. View of a prefired BSAA sample in the uniaxial compression set-up during the preparation phase.

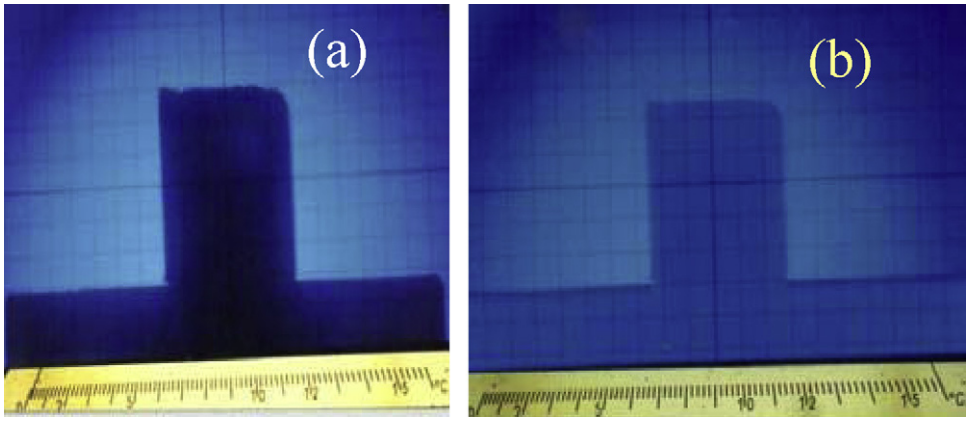

Fig. 3. Refractoriness (deformation) of BSAA samples at: (a) 20 °C and (b) 1600 °C.

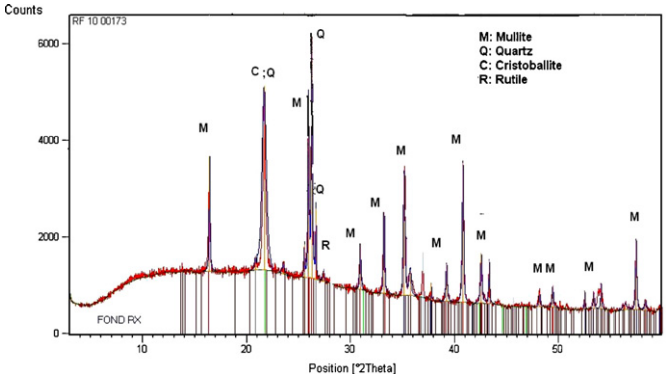

Fig. 4. XRD patterns of BSAA brick after firing at 1350 °C.

in the presence of free silica, alumina and alkaline, in accordance with the ternary SiO_2–Al_2O_3–R_2O system. DD3 clay is known for its high plasticity, which allows the introduction of a considerable quantity of inert matter (chamotte) to reduce the heating shrinkage and to ensure dimensional stability during thermal treatments. KT kaolin contains higher quartz content and a lower quantity of fine particles than DD3 clay, as well as a lower plasticity index. The incorporation of KT kaolin in the mixture enables adjustment of the physical properties of the fired material.

Refractoriness of a material is strongly dependent on microstructural parameters such as grain size and shape, the relative volume of solid and vitreous phases, the viscosity of the vitreous phase, and sample porosity [14,21]. Refractoriness can be evaluated by examining the evolution of the morphology of test samples with increasing temperature under their own weight (without any other load). Refractoriness in this paper is defined as the temperature corresponding to the moment when a material begins to lose its shape (melting point). As can be clearly seen in the photos presented in Fig. 3, the samples tested here maintained their shape without undergoing any deformation up to 1600 °C.

The main crystalline phases identified by XRD after samples were fired at 1350 °C were mullite, quartz, cristobalite and rutile (Fig. 4). The SEM micrograph of Fig. 5 clearly shows the mullite phase identified by its needle like shape. It is well known that the reactions between free silica and alkaline, in particular potassium oxide that is present in excess in the Tamazert kaolin, lead to the formation of a vitreous phase that governs the thermo-mechanical behaviour of the materials. Mullite results from the transformation of phyllosilicate minerals such as kaolinite, hallohysite and muscovite at high temperatures according to the following reactions [1,19]:

$$* \text{Kaolinite}[Al_2O_3\ 2SiO_2\ 2H_2O] \xrightarrow{450\ ^\circ C} \text{Metakaolinite}[2Al_2O_3\ 3SiO_2] \xrightarrow{980\ ^\circ C} SiO_2 + 2Al_2O_3\ 3SiO_2$$

$$\xrightarrow{1100-1200\ ^\circ C} SiO_2 + \text{Mullite}[3Al_2O_3\ 2SiO_2]$$

$$*\text{Muscovite}[K_2O\ \ 3Al_2O_3\ 6SiO_2\ 2H_2O] \xrightarrow{1200\ ^\circ C} \text{Mullite} + \text{Silica-potassium rich glassy}$$

A previous study [3] showed that excess silica in the raw materials mixture partially transforms to cristobalite beginning at 1300 °C, and then becomes totally amorphous after firing at 1400 °C. The various silica phases that compose the fired material do not have the same thermal expansion coefficient

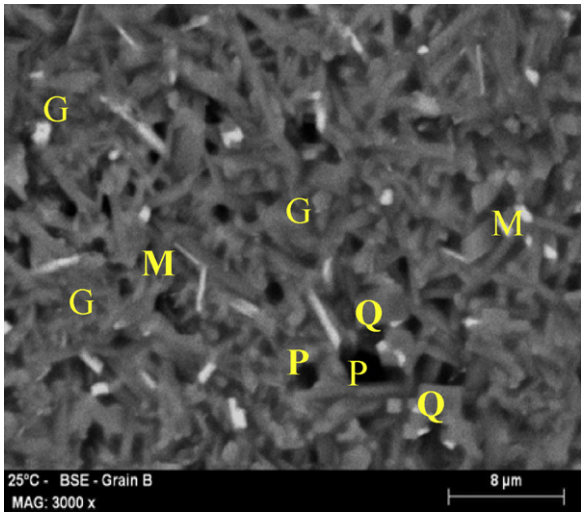

Fig. 5. SEM micrograph of a BSAA refractory brick (halloysite and KT kaolin brick) fired at 1350 °C (M: Mullite needles; Q: Quartz; G: Amorphous phase; P: Pores).

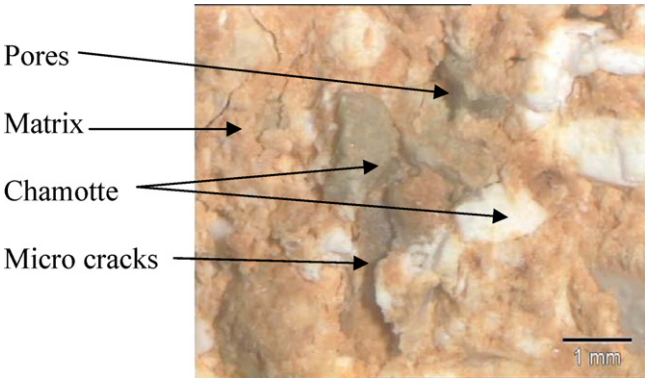

Fig. 6. Microstructure of a BSAA brick fired at 1350 °C.

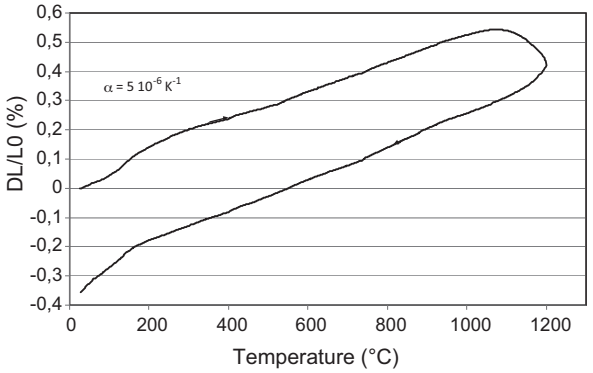

Fig. 8. Thermal expansion in air measured from room temperature to 1200 °C for 1350 °C prefired BSAA samples.

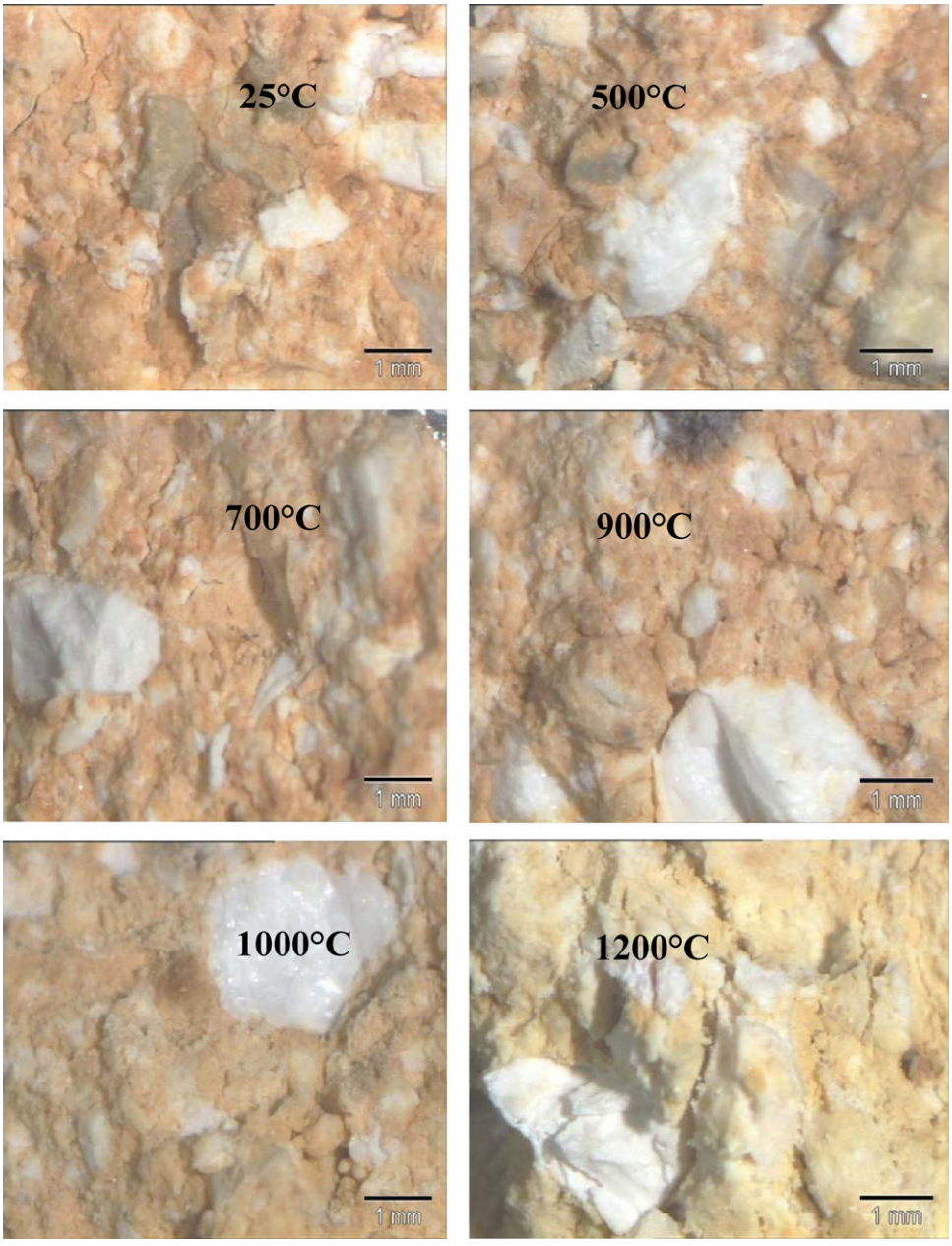

Fig. 7. Fracture surface, at room temperature of 1350 °C prefired BSAA samples after 3 point strength measurements from 25 °C to 1200 °C.

value depending on the firing temperature. Furthermore, the α–β quartz transformation at 570 °C is accompanied by a significant variation in volume [1,14]. This leads to a marked crack development around the grog grains (chamotte grains) in the matrix due to large tensile hoop stresses during sample cooling. As can be clearly seen in the photo of Fig. 6, cracks and elongated pores are observed at interfaces between grog grains and the matrix. Fig. 7 illustrates the heterogeneous character of the sample microstructure by optical micrographs, indicating

Table 7
Mean thermal expansion coefficient of BSAA bricks prefired at 1350 °C vs. temperature.

Temperature (°C)	Thermal expansion (10^{-6}/°C)
200	6.66
400	5.78
600	5.68
800	5.51
1000	5.91

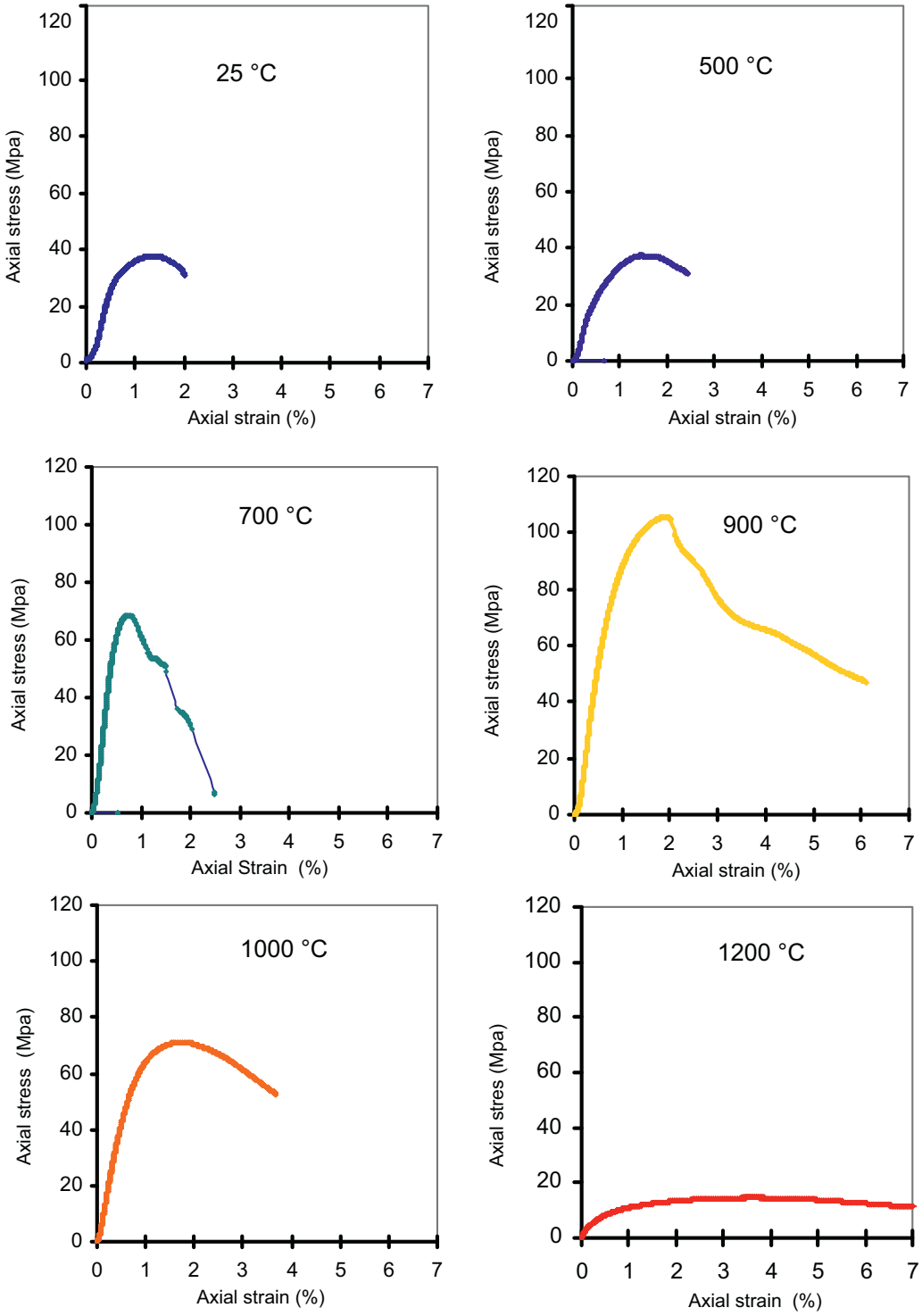

Fig. 9. Stress–strain uniaxial compression diagrams for 1350 °C prefired BSAA samples at different testing temperatures: 25, 500, 700, 900, 1000, 1200 °C.

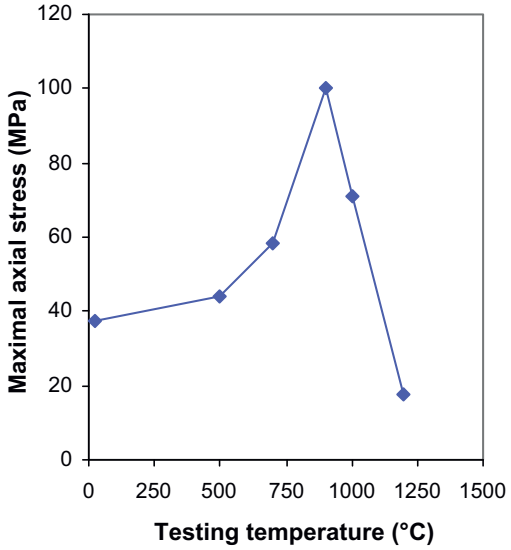

Fig. 10. Evolution of the material compression strength vs. testing temperature for 1350 °C prefired BSAA samples.

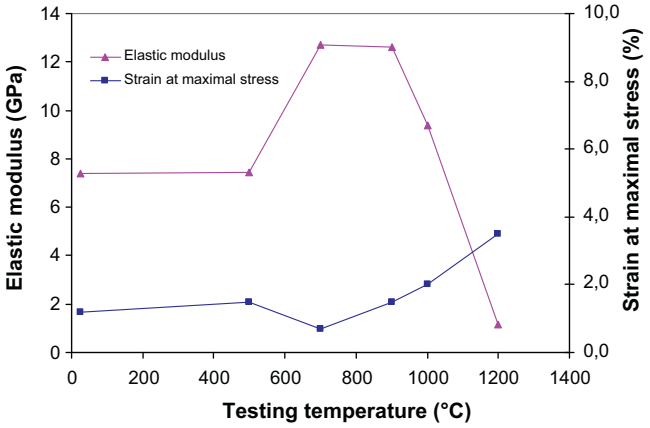

Fig. 11. Dependence of the mean value of the material's Young's modulus and the strain at maximal compressive stress vs. testing temperature for 1350 °C prefired BSAA samples.

the fractured surface of samples at the different test temperatures.

Dilatometric measurements up to 1200 °C in air were conducted on samples cut from the prefired BSAA bricks. As shown in Fig. 8, the dilatometric curve of the material is characteristic of a silica alumina refractory with high alumina content (greater than 40%) [1]. Mean thermal expansion coefficients during heating (α) were calculated and are reported in Table 7. The evolution of (α) was noted to have a marked increase from 20 °C to 200 °C then through 300 °C, that indicated the presence of cristobalite, whose α–β transformation occurs between 170 °C and 300 °C. Consistent expansion behaviour was observed from 300 to 1200 °C, leading to stability in the thermal expansion behaviour of the bricks. Because of the permanent volume change due to the cristobalite phase change, the cooling rate must be adjusted when the material is used as kiln furniture. In general, α values were similar to those of corresponding commercial alumina silicate refractory bricks (ranging from 4.5 to 8.5×10^{-6} °C^{-1}) [11,22].

Thermal shock testing was conducted on whole bricks. After samples were subjected to 15 thermal shock cycles of heating at 950 °C followed by water quenching, test brick damage was quantified by evaluating open porosity. The increase in porosity was not greater than 2% for any test sample. This constitutes satisfactory brick behaviour where abrupt temperature changes might occur.

3.2. Thermo-mechanical properties

Fig. 9 plots the stress/strain curves of compression tests carried out at various temperatures on fired BSAA refractories. The curves have bell-shape forms characteristic of quasi-brittle materials [23,24]. During testing, materials endure a maximal stress (resistance), and then lose those stresses because of high temperature material softening during heating. Successive losses of resistance are observed after the peak at 700 °C. The strain reached when the stress is a maximum (strain at peak stress) indicates the ability of a material to deform before collapsing, thus corresponding to something like ductility [25]. Fig. 10 presents the maximal stress reached at the various testing temperatures, which are values averaged from three tests at each temperature. The maximal stress increases with increasing temperature up to a maximum value at 900 °C, then decreases at higher temperatures. Fig. 11 displays the evolutions with temperature of material's elasticity modulus and strain values recorded at peak stress. The modulus of elasticity (Young's modulus) has been calculated using the stress–strain curve by measuring the slope of the linear part of the curve from 10 to 30% of the maximal stress. The recorded values are the average values of three tests at each temperature. The Young's modulus is constant at low temperatures, reaches a maximum from 700 to 900 °C, and then decreases sharply with increasing temperature. This evolution evokes that of alumina refractory concrete [24], and is slightly different from results on kaolinitic clay mixtures reported by Kolli [11], where the Young's modulus was constant at low to intermediate temperatures before decreasing at higher temperatures. The Young's modulus values in Fig. 11 are low compared to those of pure dense ceramics, which can be explained by the presence of porosity and the multiphase composition of other phases present in the samples. Part of this difference could also be due to an overestimation of the specimen height variation due to the specimen residual parallelism defects, leading to an underestimation of the Young's modulus. However, the values measured are of the same order and are consistent with numbers reported in comparable studies. For instance, an 8 GPa value was obtained at room temperature in this study instead of the 9 GPa obtained by Kolli [11] at the same firing temperature for comparable mixtures. Hence, the modulus values obtained in this study seem to be low, as they are less than 10 GPa at temperatures under 600 °C, but similar to values obtained by others at higher temperatures. The sharp decrease in the

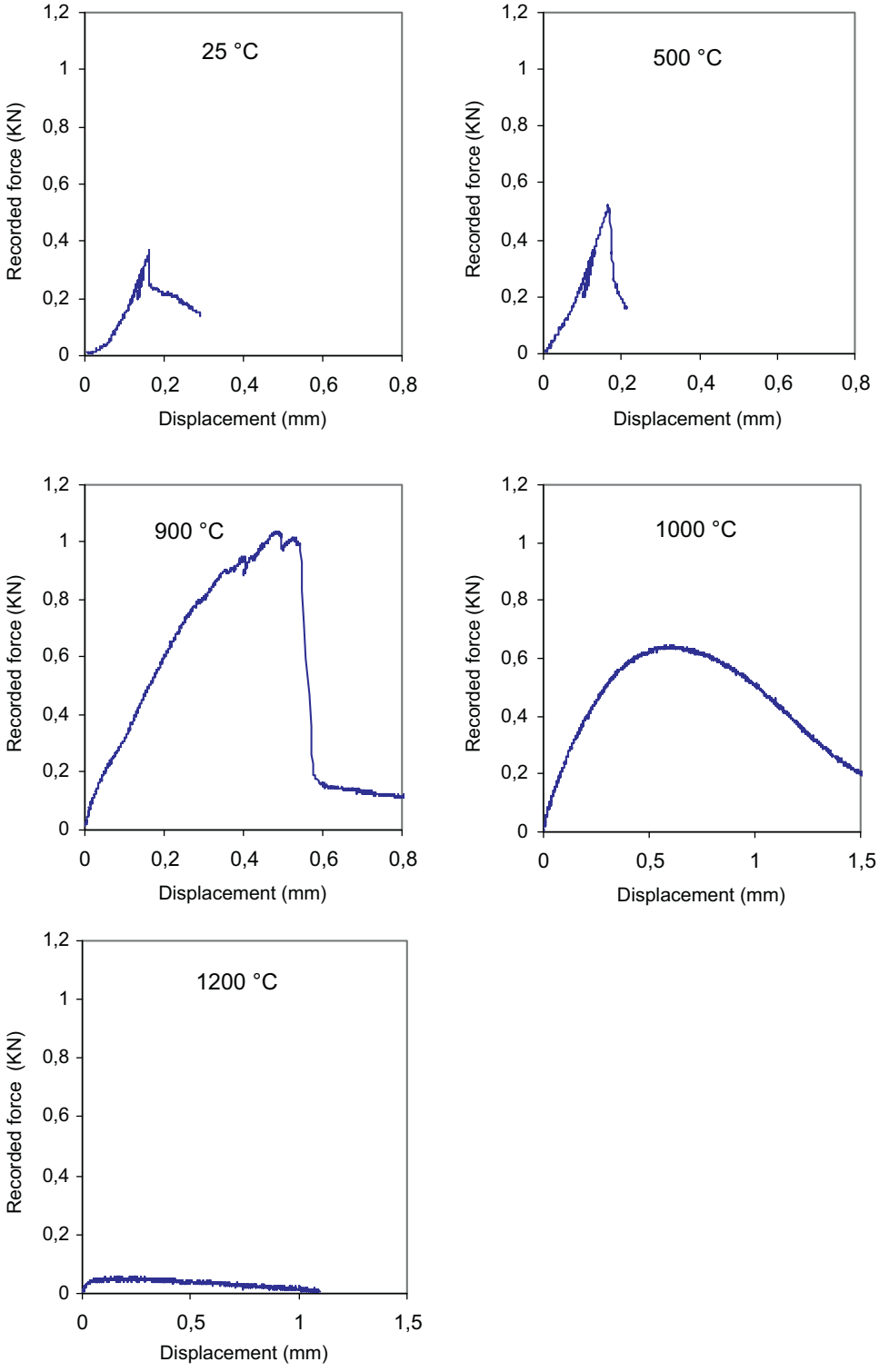

Fig. 12. Force–displacement curves during three-point bending tests for 1350 °C prefired BSAA samples at different testing temperatures.

modulus of elasticity above 900 °C in this study is similar to the work by Kolli.

The decrease of the modulus of elasticity at high temperature and the stable values at low temperature can be explained. At room temperature (after firing), the weak modulus is due to internal damage induced by the thermal expansion mismatches between phases that occurs during the cooling. When the temperature increases to 900 °C, the material absorbs the initial damage because the residual stresses due to thermal expansion mismatch decrease gradually, leading to a progressive increase in Young's modulus [22]. The viscous phase begins to appear at 900 °C and above, accelerating the material deformation, leading to a decrease of the Young's modulus.

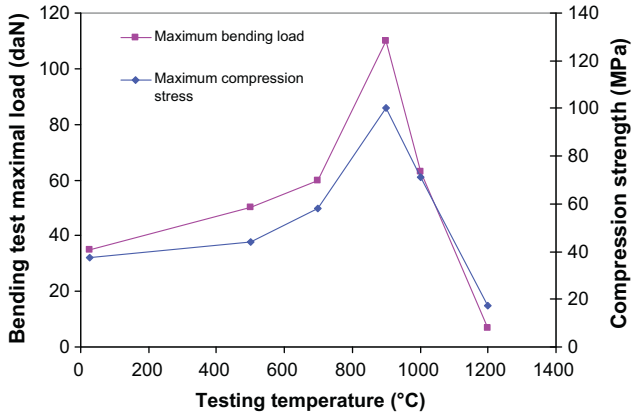

Fig. 13. Evolution of the maximal bending load and maximal compressive stress vs. testing temperature for 1350 °C prefired BSAA samples.

Fig. 11 also presents the strain reached at maximal stress. This parameter reached a minimum at 700 °C, followed by an increasing trend at higher temperatures. The minimum observed at 700 °C is characteristic, and seems to be a consequence of a healing of the material matrix, leading to the decrease of the strain at maximal stress.

Fig. 12 illustrates the results of the three-point bend tests performed at various temperatures, which were similar to results for compression tests, particularly with regard to the change of behaviour between 700 and 900 °C characterised by an increase of the strain before failure occurs. As we are interested in studying the occurrence of damage in the material, we focused on materials changes in samples that could explain observed physical property changes in the desired temperature ranges. Bending test specimens were cut from commercial processed bricks using a diamond saw, a process that might generate surface micro-cracks in the material. Although the specimen contact areas were fixed, defects in the sample preparation may have led to an overestimation of deflection measurements, causing tensile strength measured by three-point bending tests to be lower. These changes are not thought to have a major impact on results because our interest focused on changes in strength of the material behaviour with increasing temperature. If the formation process had an influence, it would have been the same for all specimens. The occurrence of viscous phases in samples at high temperatures, however, tends to minimise geometrical defects.

From 20 to 500 °C, possibly as high as 700 °C, material behaviour is brittle, with an abrupt failure occurring once tensile resistance was reached (Fig. 12). A post-peak domain is present, with the post-peak stress gaps evolving differently at each test temperature. At 900 °C, for instance, the evolution of the load before its peak is strongly non-linear, contrary to observations at lower temperatures. However, once the peak was reached, the failure was severe, and the material resistance to failure falls to a very low value, contrary to the relatively progressive decline at lower temperatures. It seems that once the macro-crack initiates at 900 °C, it propagates directly through the material, whereas at lower temperatures it remains constrained, leading to a progressive loss of resistance. Hence, in terms of microstructure interpretation, the material fracture seems to be inter-granular at low and intermediate temperatures, rather than trans-granular at 900 °C (Fig. 7). This behaviour is consistent with existing material microstructure: inter-granular micro-cracks created by the previous cooling phase are present at low temperatures, tending to be reduced and even eliminated with increasing temperature due to thermal expansion. For higher temperatures (1000–1200 °C), the load–displacement curve has an open bell-shape form that indicates the presence of the viscous phase [11,23,25]. At 1200 °C, the material resistance becomes very low, as the curve in Fig. 12 indicates.

Fig. 13 represents the variation of the maximum load with the testing temperature superimposed with the evolution of compressive strength vs. temperature. The general trend of the two curves is similar, with maximum of both strengths at 900 °C. This behaviour indicates that mechanisms driving the coalescence of micro-cracks to form macro-cracks are similar, and are of the same nature in tension and in compression. It is important to note that no new phases appear during heating at temperatures lower than the firing temperature.

4. Conclusion

Silica–alumina refractory materials made from such halloysite and kaolin clays are widely used in the manufacture of ceramic products (as kiln furniture and bricks). Because use of these materials is limited at high temperature, knowledge of their thermo-mechanical and deformation properties in fired refractory materials is necessary. Thus, mechanical tests related to modulus of rupture and crushing strength were carried out from 25 °C to 1200 °C using Algerian halloysite and kaolin clays, as well as a study of microstructure changes occurring in these compositions. From these studies, the following conclusions were drawn:

- The material's thermo-mechanical behaviour, evidenced by the compression tests and confirmed by the bending tests carried out in the temperature range of 25–1200 °C, evolved from quasi-brittle damageable at room temperature to visco-plastic damage between 900 and 1000 °C.
- The global trend of the material compression resistance vs. temperature is similar to that of tensile resistance: the maximal stress increases with temperature up to a maximum value at 900 °C, then decreases at higher temperatures.
- Optical and SEM micrographs of the fracture surfaces after heating at different temperatures revealed highly heterogeneous microstructures. Special attention should be paid to the amount of kaolin clay, in a composition which is highly siliceous. Indeed, allotropic transformations of free silica are well known to induce interfacial cracks leading to a decrease in some mechanical properties. This behaviour may explain the weakening of the Young's modulus values at low temperatures.
- Dilatometric tests show a slight and regular variation of the thermal expansion coefficient between of 300 and 1100 °C, which helps to provide a good thermal shock resistance to the material.

References

[1] G. Aliprandi, Matériaux réfractaires et céramiques techniques, Septima, Paris, 1979, pp. 1–612.

[2] P. Lapoujade, Traité pratique sur l'utilisation des produits réfractaires, H. Vial, Vial, Paris, 1986, p. 236.

[3] G.N. Djangang, A. Elimbi, U.C. Melo, G.L. Lecomte, C. Nkoumbou, J. Soro, J.P. Bonnet, P. Blanchart, D. Njopwouo, Sintering of clay – chamotte ceramic composites for refractory bricks, Ceram. Int. 34 (2008) 1207–1213.

[4] F.A.C. Minlheiro, M.N. Freire, A.G.P. Silva, J.N.F. Holanda, Densification behaviour of red firing Brazilian kaolinitic clay, Ceram. Int. 31 (2005) 757–763.

[5] M. Lalithambika, Fireclay bricks from Kerala clays, Interceramics 6 (1988) 17–19.

[6] M. Dondi, M. Marsigli, I. Ventury, Microstructure and mechanical properties of clay bricks: comparison between fast firing and traditional firing, Br. Ceram. Trans. 98 (1) (1999) 12–18.

[7] C.N. Djangang, A. Elimbi, U.C. Melo, G.L. Lecomte, C. Nkoumbou, J. Soro, J. Yvon, P. Blanchart, D. Njopwouo, Refractory ceramics from clays of Mayouom and Mvan in Cameroon, Appl. Clay Sci. 39 (2008) 10–18.

[8] K.S. Madziasni, L.M. Brown, Synthesis and mechanical properties of stoichiometric aluminium silicate (mullite), J. Am. Ceram. Soc. 55 (11) (1972) 548–552.

[9] M.A. Sainz, F. Serrano, J.M. Amigo, J. Bastida, A. Caballero, XRD microstructural analysis of mullites obtained from kaolinite–alumina mixtures, J. Eur. Ceram. Soc. 20 (2000) 403–412.

[10] I. Ganesh, J.M.F. Ferreira, Influence of raw material type and of the overall chemical composition on phase formation and sintered microstructure of mullite aggregates, Ceram. Int. 35 (2009) 2007–2015.

[11] M. Kolli, M. Hamidouche, G. Fantozzi, J. Chevalier, Elaboration and characterization of a refractory based on Algerian kaolin, Ceram. Int. 33 (2007) 1435–1443.

[12] B. Amrane, Etude d'un projet de production de briques réfractaires silico-alumineuses à base de matières premières locales, Mémoire d'Ingénieur, Université de Boumerdès, Algérie, 1993.

[13] A. Chakri, Elaboration et caractérisation des briques réfractaires de chamotte à partir des matières premières locales, Thèse de Magistère, Université de Sétif, Algérie, 1995, pp. 125–132.

[14] C. Jouenne, Traité de céramiques et de matériaux minéraux, Ed. Septima, Paris, 1975, p. 268.

[15] N orme DIN 51 730.

[16] N orme DIN 51 068.

[17] S. Djaknoun, E. Ouedraogo, A. Ahmed Benyahia, Fracture thoughness of high performance concrete on three-point bending notched beam at elevated temperature, Adv. Mater. Res. 89–91 (2010) 159–164.

[18] M. Hajjaji, S. Kacim, M. Boulmane, Mineralogy and firing characteristics of a clay from the valley of Ourika (Morocco), Appl. Clay Sci. 21 (3/4) (2002) 203–212.

[19] M. Hamidouche, M.A. Madjoubi, K. Loucif, H. Osmani, M. Kolli, M. Gonon, G. Fantozzi, Processing and characterization of refractory made of Algerian kaolin, in: Proceedings of the Eighth Conference on Ceramics, INSA de Lyon, France, 3–5 September, 2002.

[20] M. Hamidouche, M.A. Madjoubi, K. Loucif, H. Osmani, M. Kolli, M. Gonon, G. Fantozzi, Etude de la transformation de 3 nuances de kaolin en fonction de la température, Silic. Indus. 65 (11–12) (2001) 119–124.

[21] M.J. Ribeiro, J.A. Labrincha, Properties of sintered mullite and cordierite pressed bodies manufactured using Al-rich anodising sludge, Ceram. Int. 34 (2008) 593–597.

[22] B. Coope, An Introduction to Refractories, Raw Materials for the Refractories Industry, 2nd ed., Industrial Materials, 1986.

[23] J. Lemaitre, J.L. Chaboche, Mécanique des materiaux solides, 2eme ed., Dunod, Paris, 1996.

[24] E. Ouedraogo, N. Prompt, High temperature mechanical characterisation of an alumina refractory concrete for Blast Furnace main through. Part II: material behaviour, J. Eur. Ceram. Soc. 28 (2008) 2867–2875.

[25] M. Roosefid, E. Ouedraogo, N. Prompt, A. Miras, Caractérisation et modélisation du comportement thermomécanique de bétons réfractaires silico-alumineux, in: 17ème Congrès Français de Mécanique (CFM 2005), Troyes, Septembre, 2005.